Journal of Zhejiang University-SCIENCE B (Biomedicine & Biotechnology) 2023 24(8):711-722
www.jzus.zju.edu.cn; www.springer.com/journal/11585
E-mail: jzus_b@zju.edu.cn

Research Article
https://doi.org/10.1631/jzus.B2300181

Composite B-cell and T-cell lymphomas: clinical, pathological, and molecular features of three cases and literature review

Xueli JIN[1*], Hui LIU[2*], Jing LI[3], Xibin XIAO[1], Xianggui YUAN[1], Panpan CHEN[1], Boxiao CHEN[4], Yun LIANG[1✉], Fengbo HUANG[2✉]

[1]*Department of Hematology, the Second Affiliated Hospital, School of Medicine, Zhejiang University, Hangzhou 310009, China*
[2]*Department of Pathology, the Second Affiliated Hospital, School of Medicine, Zhejiang University, Hangzhou 310009, China*
[3]*Department of Nuclear Medicine, the Second Affiliated Hospital, School of Medicine, Zhejiang University, Hangzhou 310009, China*
[4]*School of Medicine, Zhejiang University, Hangzhou 310029, China*

Abstract: Composite lymphoma (CL) involving B-cell lymphoma and T-cell lymphoma is extremely rare. Herein, we report three such cases using immunohistochemistry, flow cytometry, and the next-generation sequencing (NGS) to identify the pathological and molecular characteristics of CL. In the first case, the patient was admitted to hospital for generalized pruritic maculopapular rash over the whole body. An excisional biopsy of the skin lesions showed T-cell lymphoma. At the same time, the staging bone marrow (BM) biopsy revealed a diffuse large B-cell lymphoma (DLBCL). After R-CHOP (rituximab, cyclophosphamide, doxorubicin, vincristine, and prednisone) therapies, the patient produced a good response with substantial dissipation of the rashes and relief of skin. The other two patients were admitted to hospital due to lymphadenopathy and were diagnosed with DLBCL and follicular lymphoma (FL) after core needle biopsy of lymph nodes, BM biopsy, BM aspiration, and flow cytometry. Following R-CHOP and R-COP (rituximab, cyclophosphamide, vincristine, and prednisone) therapies, they achieved complete remission unconfirmed (CRu) and complete remission (CR). However, one or two years later, they suffered a relapse of lymphadenopathy. The shocking fact was that re-biopsy of lymphadenopathy revealed peripheral T-cell lymphoma (PTCL) and angioimmunoblastic T-cell lymphoma (AITL). NGS findings identified DNA methyltransferase 3a (*DNMT3a*), isocitrate dehydrogenase 2 (*IDH2*), Ras homolog gene family, member A (*RHOA*), splicing factor 3B subunit 1 (*SF3B1*), and tumor protein p53 (*TP53*) mutations. After immunochemotherapy, these patients achieved CRu and CR again. Nevertheless, they suffered a second relapse of T-cell lymphoma. Finally, they died due to progression of disease. We found that the occurrence of CL is associated with Epstein-Barr virus infection and *DNMT3a*, *IDH2*, and *TP53* mutations, and the prognosis of the disease is closely related to the T-cell lymphoma components.

Key words: Composite lymphoma; B-cell lymphoma; T-cell lymphoma

1 Introduction

Composite lymphoma (CL) contains two or more clonally distinct types of lymphoma within the same patient. It is a very rare condition, with 1%–4% of all reported lymphoma cases (Thirumala et al., 2000; Küppers et al., 2014). Custer (1954) described the simultaneous occurrence of two or more morphological forms of Hodgkin or non-Hodgkin lymphoma within the same biopsy as the term "composite lymphoma." Rappaport et al. (1956) modified this term. Kim et al. (1977) further refined it, and since this time, a variety of different types of CLs have been described. Cases with two different histological types of lymphoma presenting sequentially are also classified as CL (Küppers et al., 2014); however, when a low-grade (indolent) lymphoma develops into a high-grade (aggressive) type, it is a lymphoma transformation and cannot be defined as CL.

The predilection sites for CL are lymph nodes or other lymphoid organs, whereas in a minority of cases, the coexisting B-cell and T-cell neoplasms arise in

✉ Yun LIANG, liangyun@zju.edu.cn
Fengbo HUANG, 2515183@zju.edu.cn
* The two authors contributed equally to this work
Xueli JIN, https://orcid.org/0000-0001-5618-920X
Yun LIANG, https://orcid.org/0000-0002-9215-1708
Fengbo HUANG, https://orcid.org/0000-0002-5548-3156

Received Mar. 16, 2023; Revision accepted Apr. 16, 2023; Crosschecked July 27, 2023

extranodal tissues (Whitling et al., 2013; Küppers et al., 2014). Histologically, most reported lymphoma subtypes found in cases of CL can be quite varied, including the combinations of essentially all major types of lymphoma. CL can be composed of a Hodgkin lymphoma component and a non-Hodgkin lymphoma component, or two distinct non-Hodgkin lymphoma components. The most frequent cases are characterized by both Hodgkin and non-Hodgkin lymphomas, or two distinct types of B-cell lymphoma (Whitling et al., 2013). Perhaps partly because of the low prevalence of T-cell lymphoma, CL cases containing both T-cell and B-cell lymphomas are very rare (Cleary and Sklar, 1984; Wolfe and Borowitz, 1984). In addition, despite cumulative evidence attained from the growing number of published case studies, the pathogenesis for developing CL remains unclear.

We herein report three cases of CL involving concurrent B-cell and T-cell lymphomas, which were positive for Epstein-Barr virus (EBV) DNA in two patients and the mutations of genes involving DNA methyltransferase 3a (*DNMT3a*), isocitrate dehydrogenase 2 (*IDH2*), Ras homolog gene family, member A (*RHOA*), splicing factor 3B subunit 1 (*SF3B1*), and tumor protein p53 (*TP53*).

2 Materials and methods

2.1 Histological and immunohistochemical analyses

All fresh tissue samples were fixed in 10% (0.10 g/mL) buffered formalin and paraffin-embedded according to routine procedures. Formalin-fixed, paraffin-embedded (FFPE) sections were cut at 4-μm thickness and stained with hematoxylin-eosin (HE) for morphologic evaluation. Immunohistochemical staining was performed using the EnVision method (Kämmerer et al., 2001), with heating in a rice cooker to repair the antigen. We purchased commercially available antibodies for the following antigens and applied them at the dilutions suggested by the manufacturers: cluster of differentiation 3 (CD3), CD4, CD5, CD7, CD8, CD10, CD15, CD19, CD20, CD23, CD30, CD43, CD45, CD56, CD79a, B-cell lymphoma 2 (BCL2), BCL6, Myc, multiple myeloma oncogene 1 (MUM1), Ki67, Granzyme B, cyclin D1, and programmed death-1 (PD-1) (Beijing Zhongshan Jinqiao Biotechnology, Beijing, China).

2.2 Flow cytometry

Flow cytometry was performed using a BD FACSCanto II cytometer, and subsequent analysis was carried out using the BD FACSDiva software (Becton Dickinson Biosciences, San Jose, CA, USA). The antibodies in the panel included those against human leukocyte antigen-DR (HLA-DR), CD2, CD3, CD4, CD5, CD7, CD8, CD10, CD11c, CD13, CD14, CD16, CD19, CD20, CD22, CD23, CD25, CD33, CD34, CD38, CD45, CD56, CD71, CD103, CD117, CD200, fast-migrating cerebrosides 7 (FMC-7), sKappa, sLambda, cKappa, cLambda, BCL2, T cell receptor αβ (TCRαβ), and TCRγδ (Becton Dickinson Biosciences).

2.3 Next-generation sequencing

Acornmed Biotechnology (Tianjin, China) was responsible for the next-generation sequencing (NGS) as a centralized clinical testing center. Based on the NGS of targeted capture, the mutation hotspots or entire coding regions of 196 genes known to mutate frequently in hematological malignancies were sequenced.

Briefly, genomic DNA was extracted from tumor FFPE tissues. After de-paraffinization with xylene and ethanol, the genomic DNA was extracted with the genomic DNA extraction kit (Qiagen, Hilden, Germany) following the manufacturer's instructions. Library preparation for the sample was performed as previously described (Chun et al., 2018). After amplifying the captured library by polymerase chain reaction (PCR), the constructed library was sequenced by an Illumina HiSeq Xten sequencer (San Diego, CA, USA).

3 Clinical features of three cases

3.1 Case 1

A 71-year-old Chinese female patient, who was a houseperson, presented generalized pruritic maculopapular rash over her whole body in August 2020. She had no fever, night sweats, or weight loss. She lived a regular life and had no family history of genetic diseases, but had a history of hypertension and diabetes, which were well controlled by oral antihypertensive drugs and hypoglycemic agent, respectively.

The patient also presented a history of chronic viral hepatitis B, and hence oral entecavir was administered to prevent viral replication. Physical examination showed multiple rashes all over the body (Figs. 1a, 1c, 1e, and 1g). An excisional biopsy of one of the right upper arm skin lesions discovered T-cell lymphoma, with no type specificity. The EBV-encoded RNA (EBER) in situ hybridization test was negative. A positron-emission tomography/computed tomography (PET/CT) scan demonstrated increased fluorodeoxyglucose-avid uptake involving the bilateral cervical, bilateral clavicular region, bilateral axillary lymph nodes, as well as increased fluorodeoxyglucose-avid uptake in the spleen with splenomegaly. We further performed B-ultrasound of lymph nodes in the neck, clavicle, armpit, and groin, but found no lymph node enlargement. The bone marrow (BM) biopsy was done for staging, and showed a diffuse large B-cell lymphoma (DLBCL). BM flow cytometric immunophenotyping further confirmed a population of aberrant large B lymphocytes.

Therefore, the final diagnosis was CL composed of T-cell lymphoma in the skin and stage IVA DLBCL in the BM. After one cycle of chemotherapy with R-CHOP (rituximab, cyclophosphamide, doxorubicin, vincristine, and prednisone) in September 2020, the patient produced a good response with substantial dissipation of the rashes and relief of skin (Figs. 1b, 1d, 1f, and 1h). Regrettably, however, after three cycles of chemotherapy with R-CHOP completed in October 2020, the patient was lost to follow up.

3.2 Case 2

This case involved a 62-year-old Chinese male patient, who worked as a farmer. In November 2017, he presented with multiple cervical and subaxillary lymphadenopathy, and also a slight dry cough. The patient had an unexplained fever, but showed no symptoms of infection, night sweats, or weight loss. He lived a regular life, did not have diabetes or cardiovascular disease, and showed no family history of genetic disease. A core needle biopsy of a left cervical lymph node revealed DLBCL. A PET/CT scan demonstrated increased fluorodeoxyglucose-avid uptake involving the bilateral cervical, axillary, hilus of the lung, mediastinal lymph nodes, and subcutaneous lymph nodes of the chest wall (Fig. 2a). A staging BM examination showed no evidence of lymphomatous involvement. The peripheral blood EBV DNA was found to be positive.

Fig. 1 Clinical features of Case 1. The skins of the upper limbs (a, b), lower limbs (c, d), abdomen (e, f), and back (g, h) before treatment in August 2020 (a, c, e, g) and after one cycle of R-CHOP treatment in September 2020 (b, d, f, h). R-CHOP: rituximab, cyclophosphamide, doxorubicin, vincristine, and prednisone.

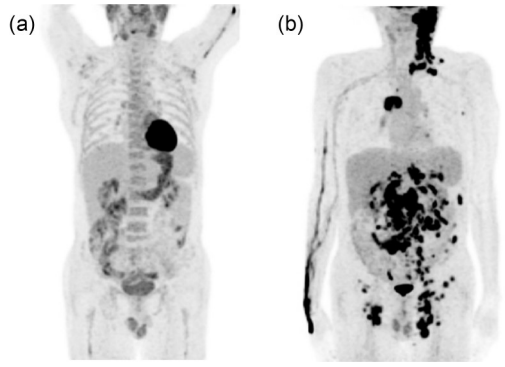

Fig. 2 PET/CT scan of Case 2. (a) PET/CT before treatment in December 2017 showed the involvement of bilateral cervical, axillary, hilus of the lung, mediastinal lymph nodes, and subcutaneous lymph nodes of the chest wall, along with increased FDG uptake; (b) PET/CT in June 2021 showed multiple lymph nodes (left retroauricular region, parotid region, neck, supraclavicular region, mediastinal 4R region, left chest wall, bilateral groin, abdominal cavity, and retroperitoneal) along with increased FDG uptake. PET: positron-emission tomography; CT: computed tomography; FDG: fluorodeoxyglucose.

The final diagnosis was stage IIB DLBCL. After six cycles of chemotherapy with R-CHOP completed in March 2018, the patient achieved complete remission unconfirmed (CRu), with the regression of superficial and mediastinal lymph nodes (Fig. 3). One year later, in May 2019, the patient presented left cervical, mediastinal, and retroperitoneal lymphadenopathy (Figs. 4a and 4c). He did not experience fevers, chills, night sweats, or significant weight loss. A subsequent core needle biopsy of a left cervical lymph node revealed peripheral T-cell lymphoma (PTCL), not otherwise specified (PTCL-NOS). Six cycles of chemotherapy with L-CHOP (lenalidomide, cyclophosphamide, doxorubicin, vinorelbine, and prednisone) were completed in October 2019. He achieved CRu again (Figs. 4b and 4d). In November 2020, the patient presented multiple lymphadenopathy in the whole body again. Core needle biopsy revealed a PTCL-NOS relapse. Subsequently, he accepted three cycles of tislelizumab and chidamide, and two cycles of tislelizumab and Gemox (gemcitabine, oxaliplatin), but did not respond well. In June 2021, PET/CT showed a progression of the disease (Fig. 2b). He was subsequently given four cycles of clinical trial (IBI322), and five cycles of azacitidine, chidamide, and lenalidomide. However, he still had a progressive disease and showed pancytopenia in April 2022. BM re-biopsy revealed T-cell lymphomatous involvement. Then, he accepted two cycles of tislelitzumab, dexamethasone, and etoposide, and two cycles of doxorubicin, pegas-pargase, and etoposide. Unfortunately, he died of disease progression in October 2022.

3.3 Case 3

The patient in this case was a retired 65-year-old Chinese male. In May 2018, he had right cervical lymphadenopathy. Core needle biopsy of the right cervical lymph node revealed grade I follicular lymphoma (FL). The patient had no fever, night sweats, or weight loss. He had a history of diabetes, which was well controlled by oral hypoglycemic drugs. The final diagnosis was stage IIA FL. He was given six cycles of chemotherapy with R-COP (rituximab, cyclophosphamide, vincristine, and prednisone) and achieved complete remission (CR). Two years later (January 2021), the patient presented left inguinal lymphadenopathy. The core needle biopsy of left inguinal lymphadenopathy revealed angioimmunoblastic T-cell lymphoma (AITL). PET/CT scan demonstrated increased fluorodeoxyglucose-avid uptake involving multiple lymph nodes above and below the diaphragm (Fig. 5a). The peripheral blood EBV DNA was found to be

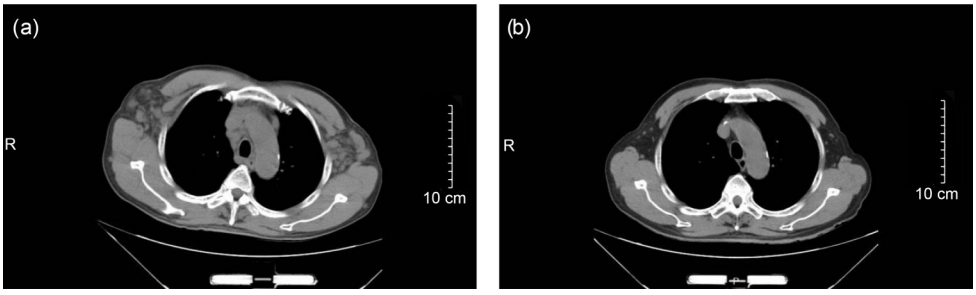

Fig. 3 Chest CT scan of Case 2. (a) Multiple axillary and mediastinal lymphadenopathy before treatment in November 2017; (b) No significant axillary or mediastinal lymph node enlargement was observed after R-CHOP therapies in May 2018. CT: computed tomography; R-CHOP: rituximab, cyclophosphamide, doxorubicin, vincristine, and prednisone.

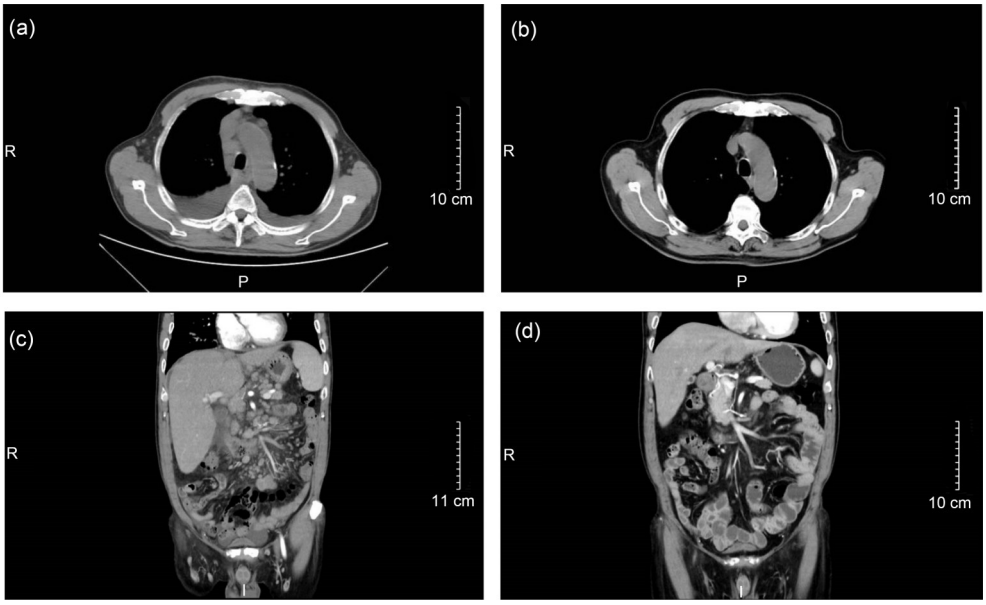

Fig. 4 Chest and abdominal CT of Case 2. (a) Multiple axillary and mediastinal lymphadenopathy before treatment in May 2019; (b) No significant axillary or mediastinal lymph node enlargement was observed after L-CHOP therapies in December 2019; (c) Multiple lymphadenopathy in the lesser omentum, mesentery, and retroperitoneum before treatment in May 2019; (d) No significant lymph node enlargement was observed in the lesser omentum, mesentery, or retroperitoneum after L-CHOP therapies in December 2019. CT: computed tomography; L-CHOP: lenalidomide, cyclophosphamide, doxorubicin, vinorelbine, and prednisone.

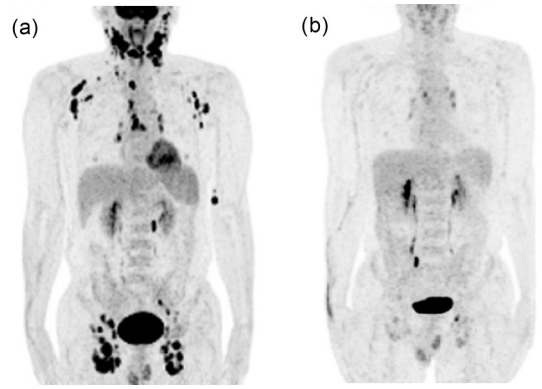

Fig. 5 PET/CT scan of Case 3. (a) PET/CT before treatment in February 2021 showed the involvement of multiple lymph nodes (left parapharyngeal, left preauricular, bilateral neck, bilateral clavicle region, bilateral armpit, mediastinum, bilateral hilum, para-aortic, bilateral internal iliac, bilateral groin, and subcutaneous soft tissue of left lower humerus) along with increased FDG uptake; (b) PET/CT after treatment in July 2021 showed that primary lesions had significantly shrunk or reduced in size, and there was no increase in FDG uptake. PET: positron-emission tomography; CT: computed tomography; FDG: fluorodeoxyglucose.

positive. The final diagnosis was AITL. He did not well respond to the GDP (gemcitabine, dexamethasone, and *cis*-platinum) therapy; therefore, he was given two cycles of azacitidine and chidamide, and three cycles of miniGemox (gemcitabine, oxaliplatin), azacitidine, and chidamide, completed in June 2021. He showed CR with a PET/CT evaluation (Fig. 5b). Seven months later (February 2022), he presented with multiple superficial lymphadenopathy and a skin itch. The core needle biopsy of the right inguinal lymphadenopathy revealed AITL relapse. He was treated with etoposide, vibutuximab, and dexamethasone. Unfortunately, he developed severe pneumonia and died of respiratory failure in March 2022.

4 Results

4.1 Histology and immunohistochemistry

4.1.1 Case 1

Excisional biopsy of the right upper arm skin lesions (August 2020) was performed, which showed T-cell lymphoma (no specific type). HE staining detected normal epidermis with elastic fiber degeneration in the superficial dermis, and the infiltration of focal irregular lymphoid cells around the blood vessels (Fig. 6a). Immunohistochemical staining revealed that the tumor cells were positive for CD3 (Fig. 6b), CD2

(Fig. 6c), CD5 (Fig. 6d), CD7, and CD8, partially positive for CD4, and scatteredly positive for Granzyme B, while negative for CD20 (Fig. 6e), CD79a, and CD10. The Ki67 proliferative index was estimated at 30% (Fig. 6f).

The BM biopsy (August 2020) revealed DLBCL. HE staining showed significant lymphocyte hyperplasia with moderate fibrosis (Fig. 7a). Immunohistochemical staining indicated that tumor cells were focally positive for CD20 (Fig. 7b) and scatteredly positive for CD3 (Fig. 7c) and CD5, myeloperoxidase (MPO) was slightly reduced, and the Ki67 proliferation index was high (Fig. 7d).

4.1.2 Case 2

Core needle biopsy of the left cervical lymph node (November 2017) revealed DLBCL, non-germinal center subtype. The tumor cells were medium to large in size and round to oval in diffuse hyperplasia with rich and lightly stained cytoplasm, the nuclei were deeply stained, and the nucleoli were visible in the center (Fig. 8a). The immunohistochemical results

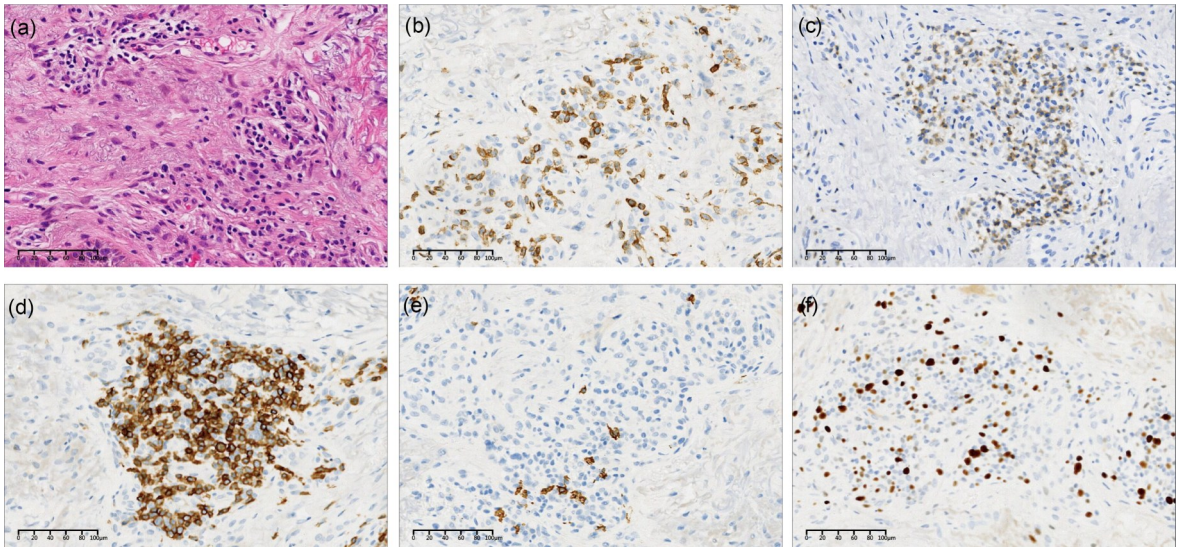

Fig. 6 Epidermis of the skin (right upper arm) of Case 1: T-cell lymphoma. (a) HE; (b–f) Immunohistochemical staining with anti-CD3 (b), anti-CD2 (c), anti-CD5 (d), anti-CD20 (e), and anti-Ki67 (f) antibodies. Scale bar=100 μm. HE: hematoxylin-eosin; CD: cluster of differentiation.

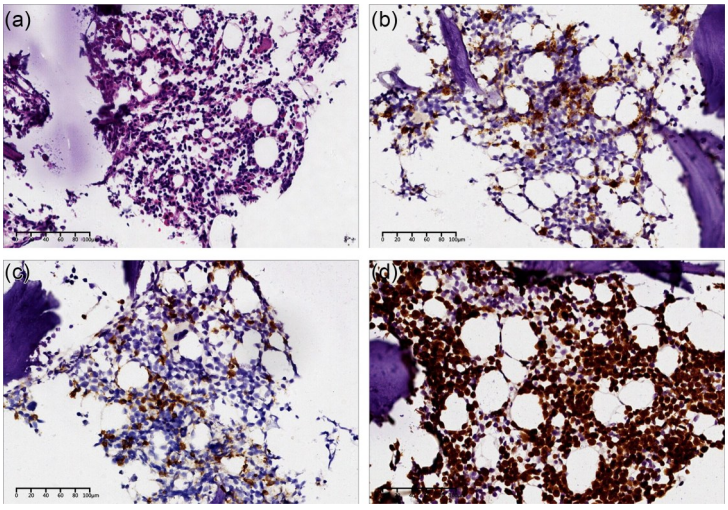

Fig. 7 Bone marrow biopsy of Case 1: diffuse large B-cell lymphoma (DLBCL). (a) HE; (b–d) Immunohistochemical staining with anti-CD20 (b), anti-CD3 (c), and anti-Ki67 (d) antibodies. Scale bar=100 μm. HE: hematoxylin-eosin; CD: cluster of differentiation.

showed that tumor cells were diffusely positive for CD20 (Fig. 8b), CD79a, and MUM1 (Fig. 8c), and negative for CD3 (Fig. 8d), CD5, CD23, and cyclin D1. The Ki67 proliferation index was up to 90% (Fig. 8e).

Core needle biopsy of the left cervical lymph node (May 2019) revealed PTCL-NOS. HE-stained sections showed the structural destruction of lymph nodes and diffuse proliferation of lymphoid cells of varying sizes, accompanied by eosinophil infiltration (Fig. 9a). The immunohistochemical results showed that the tumor cells were diffusely positive for CD3 (Fig. 9b), CD45 (leukocyte common antigen (LCA)), CD45RO, and CD5, and negative for CD20 (Fig. 9c). The Ki67 proliferation index was up to 90% (Fig. 9d).

BM re-biopsy in April 2022 revealed T-cell lymphomatous involvement. Routine sections showed active BM hyperplasia and the diffuse hyperplasia of lymphoid cells with clear cytoplasm in the BM (Fig. 10a). The immunohistochemical results showed that tumor

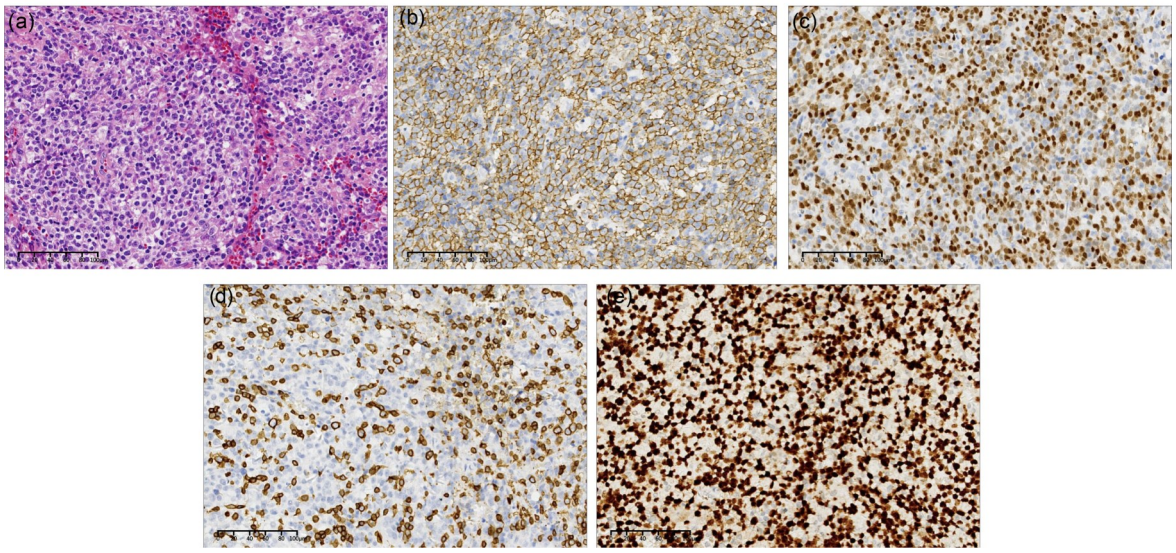

Fig. 8 Cervical lymph node of Case 2: diffuse large B-cell lymphoma (DLBCL), non-germinal center subtype. (a) HE; (b–e) Immunohistochemical staining with anti-CD20 (b), anti-MUM1 (c), anti-CD3 (d), and anti-Ki67 (e) antibodies. Scale bar=100 μm. HE: hematoxylin-eosin; CD: cluster of differentiation; MUM1: multiple myeloma oncogene 1.

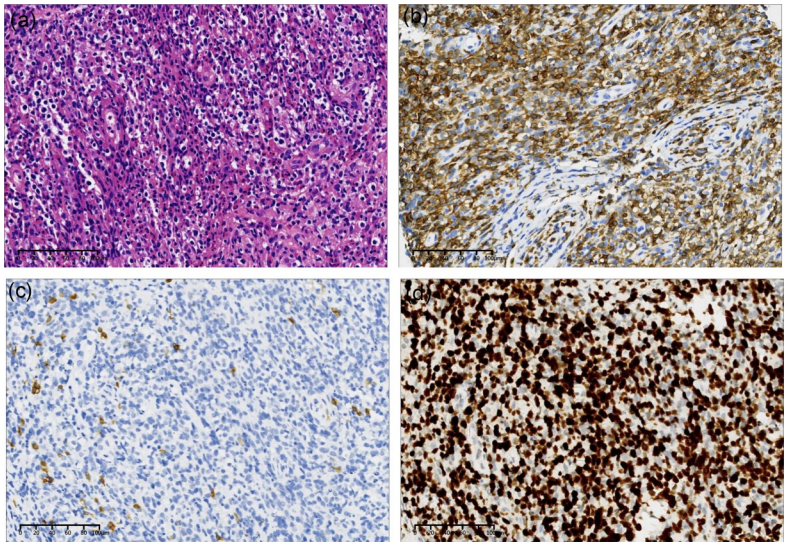

Fig. 9 Cervical lymph nodes of Case 2: peripheral T-cell lymphoma, not otherwise specified (PTCL-NOS). (a) HE; (b–d) Immunohistochemical staining with anti-CD3 (b), anti-CD20 (c), and anti-Ki67 (d) antibodies. Scale bar=100 μm. HE: hematoxylin-eosin; CD: cluster of differentiation.

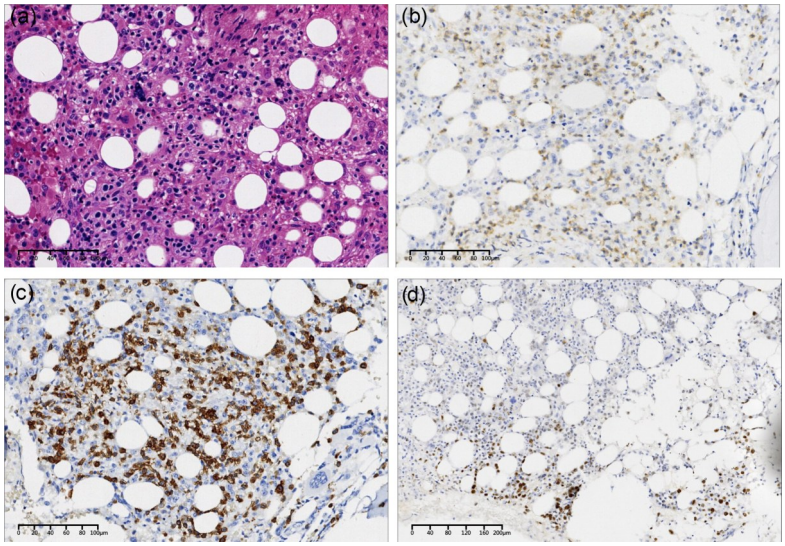

Fig. 10 Posterior superior iliac spine of Case 2: T-cell lymphoma involving bone marrow. (a) HE; (b–d) Immunohistochemical staining with anti-CD3 (b), anti-CD7 (c), and anti-Ki67 (d) antibodies. Scale bar: 100 μm (a–c) and 200 μm (d). HE: hematoxylin-eosin; CD: cluster of differentiation.

cells were positive for CD3 (Fig. 10b), CD4, and CD7 (Fig. 10c), and negative for CD20, CD79a, and terminal deoxynucleotidyl transferase (TdT). The proliferation index of Ki67 was about 10% (Fig. 10d).

4.1.3 Case 3

Core needle biopsy of the right cervical lymph node (May 2018) revealed grade I FL. The slides demonstrated the structural destruction of lymph nodes based on the lymphoid cell nodular growth pattern. The immunohistochemistry showed CD20, CD21, CD23 highlight network of follicular dendritic cells (FDCs), and BCL6 highlight B-cell nodular hyperplasia. The tumor cells were diffusely positive for BCL2. The proliferation index of Ki67 was about 10%.

Core needle biopsy of the left inguinal lymphadenopathy (January 2021) revealed AITL. Immunohistochemistry showed that tumor cells were diffusely positive for CD2, CD3, CD5, CD43, and BCL2, and partially positive for CD10 and BCL6. CD23 showed irregular proliferation of FDC network. The Ki67 proliferative index was estimated at 50%.

Subsequently, core needle biopsy of the right inguinal lymphadenopathy (February 2022) revealed AITL. The lymphocytes were diffusely grown, showing mild to moderate atypia with deep nuclear staining and high branching endothelial vein hyperplasia (Fig. 11a). The immunohistochemical results showed that tumor cells were diffusely positive for CD3 (Fig. 11b), CD10 (Fig. 11c), and PD-1 (Fig. 11d). CD23 showed the irregular proliferation of FDC network (Fig. 11e). Tumor cells were negative for CD20, CD79a, and CD56. CD4 was diffusely positive in tumor cells (Fig. 11f), while CD8 (Fig. 11g) was only scattered. The Ki67 proliferative index was estimated at 40% (Fig. 11h).

4.2 Flow cytometry

In Case 1, excisional biopsy of the skin lesions revealed T-cell lymphoma. At the same time, BM biopsy showed DLBCL. To further confirm the diagnosis, BM flow cytometric immunophenotyping was performed. We found a population of aberrant large B lymphocytes comprising approximately 7.5% of total viable cellular events (Fig. 12). These were positive for CD19, CD20, CD22, CD45, sKappa (dim), cKappa (dim), and FMC-7, partially positive for CD11c and CD23, and negative for CD3, CD4, CD5, CD8, CD10, CD25, CD38, CD103, CD200, and BCL2.

4.3 Next-generation sequencing

One year after the successful initial treatment in May 2019, the patient in Case 2 suffered a re-enlargement of the cervical lymph nodes, and core needle re-biopsy was done to confirm whether the lymphoma relapsed. A surprising finding was that re-biopsy of lymphadenopathy revealed PTCL, not DLBCL. To further elucidate the molecular characteristics of

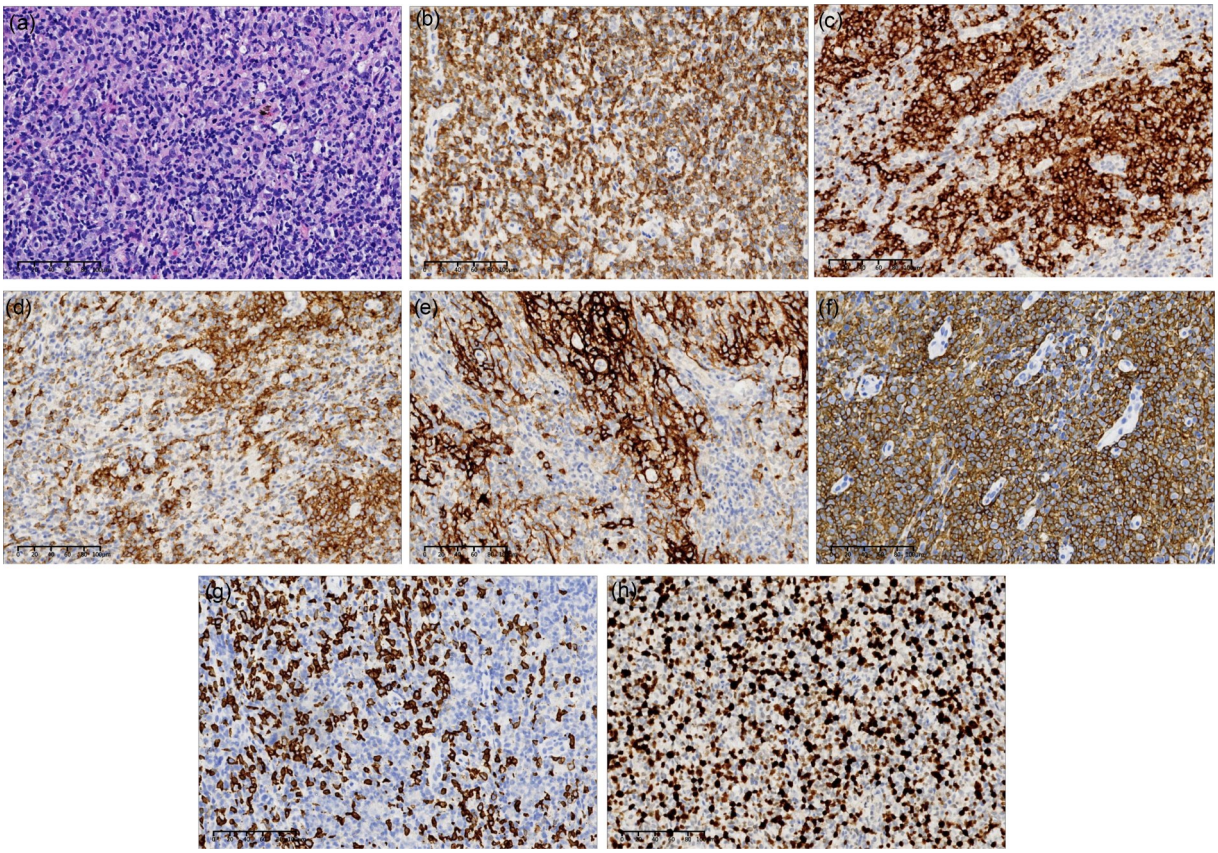

Fig. 11 Right inguinal lymph node of Case 3: angioimmunoblastic T-cell lymphoma (AITL). (a) HE; (b–h) Immunohistochemical staining with anti-CD3 (b), anti-CD10 (c), anti-PD-1 (d), anti-CD23 (e), anti-CD4 (f), anti-CD8 (g), and anti-Ki67 (h) antibodies. Scale bar=100 μm. HE: hematoxylin-eosin; CD: cluster of differentiation; PD-1: programmed death-1.

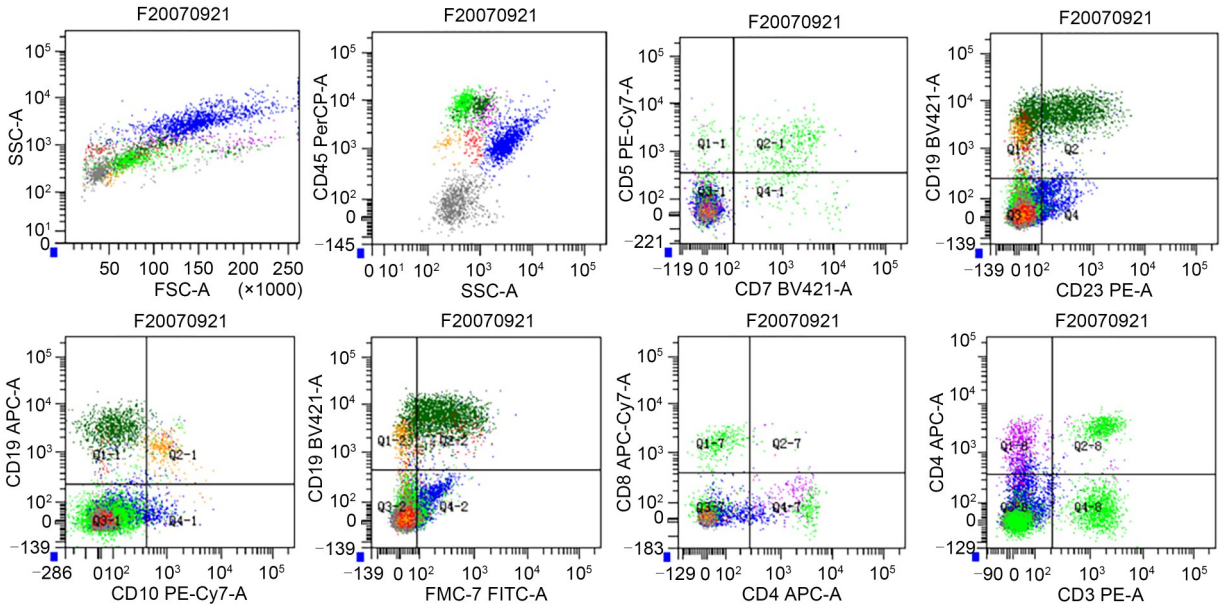

Fig. 12 Case 1: immunophenotypic analysis of the bone marrow by 8-color flow cytometry. Atrovirens events, neoplastic B lymphocytes; green events, normal lymphocytes; blue events, granulocytes; red events, blast cells; purple events, monocytes; yellow events, precursor B-cell; sky-blue events, plasmocytes; gray events, nucleated red blood cell.

the disease, the FFPE sections were sent to Acornmed Biotechnology (Tianjin, China) for NGS detection. The NGS findings identified *DNMT3a*, *IDH2*, *RHOA*, *SF3B1*, and *TP53* mutations (Table 1).

5 Discussion

The occurrence of CL is infrequent. Meanwhile, despite many reported cases in the literature, the underlying mechanism for developing CL remains unclear. Certainly, however, CL does not occur by chance. A few hypotheses for the pathogenesis of the development of CL are explained as follows.

The first possible cause might be an environmental risk factor, that is, immune dysregulation caused by the first lymphoma, engendering an environment that is conducive to the second lymphoma (Xu et al., 2002). One such example is viral infection, with EBV being the most common. In this study, Cases 2 and 3 were shown to be positive for EBV DNA at the time of the first B-cell lymphoma. EBV antigens expressed in malignant B-cells might stimulate T-cell proliferation; in certain cases, it might induce T-cell neoplastic transformation through clonal selection (Zettl et al., 2002). Alternatively, EBV in already-existing T-cell lymphoma might also be a possible etiological agent involved in the development of the B-cell component. Intrinsic immunodeficiency caused by T-cell lymphoma may cause host B-cell infection with EBV and induce B-cell transformation. However, this is not the only mechanism for the formation of CL, as many other CL cases, like Case 1 in this work, showed no evidence of EBV infection.

Immune dysregulation caused by autoimmune conditions might be another cause for the development of CL. Hu et al. (1987) described a CL patient who had a previously diagnosed autoimmune condition. Both B-cells and T-cells may be stimulated through chronic exposure to autoantigens, which might induce the transformation of both cell lineages in the process of proliferation.

Another possible explanation for the formation of CL might be that either sharing a common progenitor or being nurtured by the same microenvironment undergoing divergent evolution via additional genomic modification results in heterogeneous subclones that are capable of generating both B-cell and T-cell clones. Wang et al. (2014) showed a CL case composite mantle cell lymphoma (MCL), and PTCL demonstrated the rearrangement and replications of cyclin D1 (*CCND1*) gene and the upregulation of its protein cyclin D1 expression in both B-cell and T-cell lymphomas. Tanaka et al. (2018) reported a CL case where both B-cell and T-cell neoplasms likely arose from the follicle center with genetic alterations involving the immunoglobulin heavy chain (*IgH*) gene within each lymphoma.

At the same time, with the development of molecular technology, several molecular mechanisms may also contribute to CL development. Mutations of epigenetic regulators including DNA methylation genes *DNMT3a* and *IDH2* might induce the occurrence of a second lymphoma. DNA methyltransferase (DNMT) mediates an essential epigenetic mechanism that controls cell proliferation, apoptosis, differentiation, cell cycle, and cell transformation. A previous study found that *DNMT3a* was overexpressed in 13% of DLBCL patients (Amara et al., 2010). *DNMT3a* (5%–36%) and *IDH2* (0%–8%) have also been identified in patients with PTCL-NOS; additionally, *DNMT3a* and *IDH2* were mutated in 20%–45% and 26%–38% of AITL cases, respectively (Couronné et al., 2012; Odejide et al., 2014). Thus, under certain circumstances, *DNMT3a* mutation may lead to both B-cell and T-cell lymphomas in a single patient.

Table 1 Results of NGS in the left neck lymph node

Mutated gene	Transcript ID	Mutated site	Nucleic change	Amino acid change	VAF (%)
DNMT3a	NM_022552	Exon 19	c.2207G>A	p.R736H	23.91
IDH2	NM_002168	Exon 4	c.515G>T	p.R172M	8.59
RHOA	NM_001664	Exon 2	c.50G>T	p.G17V	10.36
SF3B1	NM_012433	Exon 14	c.1997A>C	p.K666T	1.19
TP53	NM_000546	Exon 7	c.730G>C	p.G244R	1.27

NGS: next-generation sequencing; *DNMT3a*: DNA methyltransferase 3a; *IDH2*: isocitrate dehydrogenase 2; *RHOA*: Ras homolog gene family, member A; *SF3B1*: splicing factor 3B subunit 1; *TP53*: tumor protein p53.

Trimech et al. (2021) reported a small series of patients with CLs consisting of chronic lymphocytic leukemia/small lymphocytic lymphoma (CLL/SLL) and AITL, in which the AITL comprised prominent clear cells with similar mutations consisting of tet methylcytosine dioxygenase 2 (*TET2*) or *DNMT3a* alteration. Zhang et al. (2022) also found a *DNMT3a* mutation in CL in both CLL/SLL and monomorphic epitheliotropic intestinal T-cell lymphoma (MEITL) tissues. Besides, previous studies have also shown that *TP53* mutation can be identified in both B-cells and T-cells in the lymph nodes (Xie et al., 2020; Onaindia et al., 2021; Luo et al., 2022), which might also contribute to the occurrence of CL. In our Case 2, NGS detection showed *DNMT3a* and *TP53* mutations.

Although we still have not found out the exact mechanism for the formation of CL, it is certain that the pathogenesis is complex, with more than one pathophysiologic mechanism involved in the development of CL of B-cell and T-cell origins.

Because of its low incidence, there is no standard treatment for CL. Therefore, the overall therapeutic strategies need to cover both disease components. R-CHOP or CHOP-like regimens are usually used as first-line treatments for CL of B-cell and T-cell lymphomas (Zettl et al., 2002; Balagué et al., 2007). Currently, there is no standard treatment for refractory or relapsed CL either. Therapeutic regimens should be chosen according to a necessary re-biopsy to determine whether the recurrence is only T-cell lymphoma, B-cell lymphoma, or still CL. The prognosis of patients with CL of B-cell and T-cell lymphomas varies considerably because of the heterogeneous combination of neoplastic components. Zettl et al. (2002) reported that EBV-associated B-cell lymphoproliferation occurring in AITL did not seem to be associated with a more aggressive clinical course than typical AITL clinically. Conversely, some scholars believe that CL containing both T and B neoplasms follows an aggressive clinical course. Suefuji et al. (2012) reported 19 CL patients of B-cell and T-cell lymphomas; after a median follow-up of three months (range, 1–13 months), 12 (63.2%) patients were alive and 7 (36.8%) patients had died of the disease. Two patients we reported showing that B-cell lymphoma was successfully cured with R-CHOP regimens; however, T-cell lymphoma relapsed two times and led to the death of the patients. Hence, the response of the more aggressive T-cell component to chemotherapy determines the disease prognosis. The progression free survival (PFS) of the two cases we reported was 1–2 years, and the overall survival (OS) was 4–6 years.

In conclusion, in rare circumstances, B-cell lymphoma can occur in combination with T-cell lymphoma. In our experience, physicians should not stop pursuing treatment for secondary lymphoma even if they have identified one major lymphoma. With the recent advances in diagnostic modalities, such as immunophenotyping, flow cytometry, immunohistochemistry, analytical and molecular diagnostic tests, particularly their applications in clinical practice, the detection rate of CL can be expected to increase in the future.

Data availability

The data that support the findings of this study are available on request from the corresponding author. The data are not publicly available due to privacy or ethical restrictions.

Acknowledgments

This work was supported by the Zhejiang Medical Health Science and Technology Project (No. 2021KY166) and the Natural Science Foundation of Zhejiang Province (No. LQ23H080003), China.

Author contributions

Xueli JIN and Yun LIANG performed the clinical data collection, and wrote and edited the manuscript. Hui LIU and Fengbo HUANG performed the pathological data collection. Jing LI and Boxiao CHEN performed the data collection of PET/CT. Xibin XIAO, Xianggui YUAN, and Panpan CHEN contributed to the study design, writing and editing of the manuscript. All authors have read and approved the final manuscript, and therefore, have full access to all the data in the study and take responsibility for the integrity and security of the data.

Compliance with ethics guidelines

Xueli JIN, Hui LIU, Jing Li, Xibin XIAO, Xianggui YUAN, Panpan CHEN, Boxiao CHEN, Yun LIANG, and Fengbo HUANG declare that they have no conflict of interest.

All procedures followed were in accordance with the ethical standards of the responsible committee on human experimentation (institutional and national) and with the Helsinki Declaration of 1975, as revised in 2013. The study was approved by the ethical committee of the Second Affiliated Hospital, School of Medicine, Zhejiang University (No. 2023 (0227)). Informed consent was obtained from all patients for being included in the study. Additional informed consent was obtained from all patients for whom identifying information is included in this article.

References

Amara K, Ziadi S, Hachana M, et al., 2010. DNA methyltransferase DNMT3b protein overexpression as a prognostic factor in patients with diffuse large B-cell lymphomas. *Cancer Sci*, 101(7):1722-1730. https://doi.org/10.1111/j.1349-7006.2010.01569.x

Balagué O, Martínez A, Colomo L, et al., 2007. Epstein-Barr virus negative clonal plasma cell proliferations and lymphomas in peripheral T-cell lymphomas: a phenomenon with distinctive clinicopathologic features. *Am J Surg Pathol*, 31(9):1310-1322. https://doi.org/10.1097/PAS.0b013e3180339f18

Chun SM, Sung CO, Jeon H, et al., 2018. Next-generation sequencing using S1 nuclease for poor-quality formalin-fixed, paraffin-embedded tumor specimens. *J Mol Diagn*, 20(6):802-811. https://doi.org/10.1016/j.jmoldx.2018.06.002

Cleary ML, Sklar J, 1984. Lymphoproliferative disorders in cardiac transplant recipients are multiclonal lymphomas. *Lancet*, 324(8401):489-493. https://doi.org/10.1016/s0140-6736(84)92566-2

Couronné L, Bastard C, Bernard OA, 2012. *TET2* and *DNMT3A* mutations in human T-cell lymphoma. *N Engl J Med*, 366(1):95-96. https://doi.org/10.1056/NEJMc1111708

Custer R, 1954. Pitfalls in the diagnosis of lymphoma and leukemia from the pathologist's point of view. Proceeding of the Second National Cancer Conference. American Cancer Society, New York, p.554-557.

Hu E, Weiss LM, Warnke R, et al., 1987. Non-Hodgkin's lymphoma containing both B and T cell clones. *Blood*, 70(1):287-292. https://doi.org/10.1182/blood.V70.1.287.287

Kämmerer U, Kapp M, Gassel AM, et al., 2001. A new rapid immunohistochemical staining technique using the EnVision antibody complex. *J Histochem Cytochem*, 49(5):623-630. https://doi.org/10.1177/002215540104900509

Kim H, Hendrickson MR, Dorfman RF, 1977. Composite lymphoma. *Cancer*, 40(3):959-976. https://doi.org/10.1002/1097-0142(197709)40:3<959::aid-cncr2820400302>3.0.co;2-3

Küppers R, Dührsen U, Hansmann ML, 2014. Pathogenesis, diagnosis, and treatment of composite lymphomas. *Lancet Oncol*, 15(10):e435-e446. https://doi.org/10.1016/S1470-2045(14)70153-6

Luo C, Yu T, Young KH, et al., 2022. HDAC inhibitor chidamide synergizes with venetoclax to inhibit the growth of diffuse large B-cell lymphoma via down-regulation of MYC, BCL2, and TP53 expression. *J Zhejiang Univ-Sci B (Biomed & Biotechnol)*, 23(8):666-681. https://doi.org/10.1631/jzus.B2200016

Odejide O, Weigert O, Lane AA, et al., 2014. A targeted mutational landscape of angioimmunoblastic T-cell lymphoma. *Blood*, 123(9):1293-1296. https://doi.org/10.1182/blood-2013-10-531509

Onaindia A, Santiago-Quispe N, Iglesias-Martinez E, et al., 2021. Molecular update and evolving classification of large B-cell lymphoma. *Cancers*, 13(13):3352. https://doi.org/10.3390/cancers13133352

Rappaport H, Winter WJ, Hicks EB, 1956. Follicular lymphoma. A re-evaluation of its position in the scheme of malignant lymphoma based on a survey of 253 cases. *Cancer*, 9(4):792-821. https://doi.org/10.1002/1097-0142(195607/08)9:4<792:aid-cncr2820090429>3.0.co;2-b

Suefuji N, Niino D, Arakawa F, et al., 2012. Clinicopathological analysis of a composite lymphoma containing both T- and B-cell lymphomas. *Pathol Int*, 62(10):690-698. https://doi.org/10.1111/j.1440-1827.2012.02858.x

Tanaka J, Su P, Luedke C, et al., 2018. Composite lymphoma of follicular B-cell and peripheral T-cell types with distinct zone distribution in a 75-year-old male patient: a case study. *Hum Pathol*, 76:110-116. https://doi.org/10.1016/j.humpath.2017.11.017

Thirumala S, Esposito M, Fuchs A, 2000. An unusual variant of composite lymphoma: a short case report and review of the literature. *Arch Pathol Lab Med*, 124(9):1376-1378. https://doi.org/10.5858/2000-124-1376-AUVOCL

Trimech M, Letourneau A, Missiaglia E, et al., 2021. Angioimmunoblastic T-cell lymphoma and chronic lymphocytic leukemia/small lymphocytic lymphoma: a novel form of composite lymphoma potentially mimicking Richter syndrome. *Am J Surg Pathol*, 45(6):773-786. https://doi.org/10.1097/PAS.0000000000001646

Wang ED, Papavassiliou P, Wang AR, et al., 2014. Composite lymphoid neoplasm of B-cell and T-cell origins: a pathologic study of 14 cases. *Hum Pathol*, 45(4):768-784. https://doi.org/10.1016/j.humpath.2013.11.008

Whitling NA, Shanesmith RP, Jacob L, et al., 2013. Composite lymphoma of mycosis fungoides and cutaneous small B-cell lymphoma in a 73-year-old male patient. *Hum Pathol*, 44(4):670-675. https://doi.org/10.1016/j.humpath.2012.09.014

Wolfe JA, Borowitz MJ, 1984. Composite lymphoma: a unique case with two immunologically distinct B-cell neoplasms. *Am J Clin Pathol*, 81(4):526-529. https://doi.org/10.1093/ajcp/81.4.526

Xie CQ, Li X, Zeng H, et al., 2020. Molecular insights into pathogenesis and targeted therapy of peripheral T cell lymphoma. *Exp Hematol Oncol*, 9:30. https://doi.org/10.1186/s40164-020-00188-w

Xu Y, McKenna RW, Hoang MP, et al., 2002. Composite angioimmunoblastic T-cell lymphoma and diffuse large B-cell lymphoma: a case report and review of the literature. *Am J Clin Pathol*, 118(6):848-854. https://doi.org/10.1309/VD2D-98ME-MB3F-WH34

Zettl A, Lee SS, Rüdiger T, et al., 2002. Epstein-Barr virus-associated B-cell lymphoproliferative disorders in angioimmunoblastic T-cell lymphoma and peripheral T-cell lymphoma, unspecified. *Am J Clin Pathol*, 117(3):368-379. https://doi.org/10.1309/6UTX-GVC0-12ND-JJEU

Zhang B, Zhang YY, Li Q, et al., 2022. Case report: chronic lymphocytic leukemia/small lymphocytic lymphoma and monomorphic epitheliotropic intestinal T-cell lymphoma: a composite lymphoma. *Pathol Oncol Res*, 28:1610653. https://doi.org/10.3389/pore.2022.1610653